Attempting to understand (and control) the relationship between structure and magnetism in an extended family of Mn-6 single-molecule magnets

Post-print of a peer-reviewed article published by the Royal Society of Chemistry. Published article available at: http://dx.doi.org/10.1039/B822235E

Cite as:
Inglis, R., Jones, L. F., Milios, C. J., Datta, S., Collins, A., Parsons, S., Wernsdorfer, W., Hill, S., Perlepes, S. P., Piligkos, S., & Brechin, E. K. (2009). Attempting to understand (and control) the relationship between structure and magnetism in an extended family of Mn-6 single-molecule magnets. *Dalton Transactions*, 2009(18), 3403-3412.

Manuscript received: 10/12/2008; Accepted: 23/02/2009; Article published: 17/03/2009

Attempting to Understand (and Control) the Relationship between Structure and Magnetism in an Extended Family of Mn_6 Single-Molecule Magnets**

Ross Inglis,[1] Leigh F. Jones,[1] Constantinos J. Milios,[1,6] Saiti Datta,[2] Anna Collins,[1] Simon Parsons,[1] Wolfgang Wernsdorfer,[3] Stephen Hill,[2] Spyros P. Perlepes,[4] Stergios Piligkos[5] and Euan K. Brechin[1,]*

[1]EaStCHEM, School of Chemistry, Joseph Black Building, University of Edinburgh, West Mains Road, Edinburgh, EH9 3JJ, UK.

[2]Department of Chemistry, University of Crete, Herakleion, Greece.

[3]Department of Physics, University of Florida, Gainesville, USA.

[4]Institut Néel, CNRS & Université J. Fourier, BP 166, Grenoble, France.

[5]Department of Chemistry, University of Patras, Patras, Greece.

[6]Department of Chemistry, University of Copenhagen, Universitetsparken 5, Denmark.

[*]Corresponding author; e-mail: ebrechin@staffmail.ed.ac.uk, tel: +44 (0)131-650-7545

[**]The authors would like to thank the Leverhulme Trust for funding.

Supporting information:
†Electronic supplementary information (ESI) available: Crystallographic data in tabular form. CCDC reference numbers 706507 (3), 706508 (4), 706509 (5), 706510 (8), 706504 (13), 706505 (21) and 706506 (22). For ESI and crystallographic data in CIF or other electronic format see http://dx.doi.org/10.1039/B822235E

Abstract

The synthesis and characterisation of a large family of hexametallic [Mn^{III}_6] Single-Molecule Magnets of general formula [$Mn^{III}_6O_2$(R-sao)$_6$(X)$_2$(sol)$_{4-6}$] (where R = H, Me, Et; X = ^-O_2CR (R = H, Me, Ph etc) or Hal^-; sol = EtOH, MeOH and / or H_2O) are presented. We show how deliberate structural distortions of the [Mn_3O] trinuclear moieties within the [Mn_6] complexes are used to tune their magnetic properties. These findings highlight a qualitative magneto-structural correlation whereby the type (anti- or ferromagentic) of each Mn_2 pairwise magnetic exchange is dominated by the magnitude of each individual Mn-N-O-Mn torsion angle. The observation of magneto-structural correlations on such large polymetallic complexes is rare and represents one of the largest studies of this kind.

Introduction

Studies of the magnetic behaviour of polymetallic cluster compounds have increased greatly in recent years because such species are the gateway for discovering fascinating new physics.[1] The emergence of *Molecular Nanomagnets* in proposed applications as diverse as information storage, molecular spintronics, quantum computation and magnetic refrigeration[2] has seen synthetic chemists, physicists, theoreticians and materials scientists working to create, understand and design molecules with specific properties. One successful strategy for obtaining such clusters is self-assembly using flexible bridging ligands,[3] and a class of ligands that have seen a huge resurgence recently in this respect are oximes.[4]

Phenolic oximes, with the generic structure shown in Figure. 1, have existed for decades with uses not only academically, but as industrial metal extractants and anti-corrosive agents in protective coatings.[4] Some time ago we initiated a somewhat alternative approach to making Mn^{III} cluster compounds - a project involving the use of derivatised salicyaldoximes in which we used the deliberate targeted structural distortion of pre-made/known SMMs as a means of enhancing SMM properties.[5] After the serendipitous discovery of both ferromagnetic (S=6) and antiferromagnetic (S=2) oxime-based [Mn^{III}_3O] triangles[6] we speculated that the exchange between the metals in some such systems could be controlled by the degree of twisting of the Mn-N-O-Mn moiety.[7] We decided that the way to address this question was to derivatise the oximate carbon atom with alkyl or aryl groups (R, Figure. 1), *i.e.* make Me-saoH_2, Et-saoH_2 and Ph-saoH_2 and analogues thereof on the assumption that additional steric bulk would make a planar Mn-N-O-Mn moiety *"impossible"*. In order to test our idea, we decided to remake analogues of the [$Mn^{III}_6O_2$(sao)$_6$(O_2CR')$_2$(solvent)$_4$] family of SMMs[8] replacing the 'planar' sao^{2-} ligand with the 'non-planar' R-sao^{2-} ligands.[6,7] We chose to examine the family of hexanuclear species rather than the trinuclear species because the former class of complexes promised to afford molecules with S=12 ground states and large axial zero-field splitting parameters. An advantage for this approach is the weak exchange between the MnIII centres in this class of SMMs, which is typically only a few wavenumbers

(<1-2 cm-1) in magnitude,9 meaning that the switching of an antiferromagnetic exchange to a ferromagnetic exchange interaction should be easier to achieve – since only minor structural modifications can lead to major changes in $|J|$.10

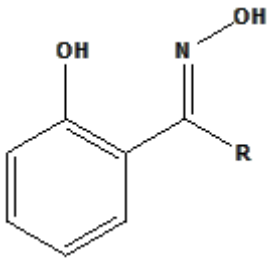

Figure 1. Structure of the phenolic oximes R-saoH_2 (R = H, saoH_2; Me, Me-saoH_2; Et, Et-saoH_2 *etc*).

Our appoach was successful[11] with the discovery that the clusters $[Mn_6O_2(Et\text{-}sao)_6(O_2CPh)_2(EtOH)_4(H_2O)_2]$ and $[Mn_6O_2(Et\text{-}sao)_6(O_2CPh(Me)_2)_2(EtOH)_6]$ both possessed S=12 ground states, the latter molecule displaying an energy barrier to magnetisation reversal of ~86 K.[6,7] Understanding, in detail, the relationship between the structure of a cluster and its magnetic properties is non-trivial (especially quantitatively) since it depends on the combination of a number of factors, but an initial study of a total of twelve members of *this* family suggested that the *dominant* factor determining the sign and strength of the exchange was the relative twisting of the Mn-O-N-Mn moiety.[11] In order to expand and enhance our previous magneto-structural correlations, we have now extended the family to twenty four members and below describe their structures and magnetic behaviour, which is summarised in Tables 1 and 2 (at the end of this document) with **1**-**24** being listed in order of increasing ground spin state *S*.

Results and Discussion

The synthesis of the clusters is straightforward:[6,7]† Reaction of a simple Mn^{II} salt (e.g. $Mn^{II}(ClO_4)_2{\cdot}6H_2O$, $MnBr_2$, $MnCl_2{\cdot}4H_2O$ *etc*) with the (derivatised) salicyaldoxime ligand R-saoH_2 (R = H, Me, Et) in alcohol (ROH, R = Me, Et) in the presence of a carboxylic acid (or the corresponding sodium salt) and a suitable base (NaOMe, NH_4OH or NEt_3) affords hexametallic complexes of general formula $[Mn^{III}{}_6O_2(R\text{-}sao)_6(X)_2(sol)_{4\text{-}6}]$ (R = H, Me, Et; X = carboxylate or halide; sol = MeOH, EtOH H_2O) in excellent yields in 2-3 days.†

All twenty four complexes display very similar molecular structures; interatomic distances and angles relevant to the discussion herein are shown in Table 1. All molecules possess an inversion centre, besides

complex **9** which lacks any molecular symmetry. They can be described (Figures. 2-3) as consisting of two parallel off-set, stacked $[Mn^{III}_3(\mu_3\text{-}O)]^{7+}$ triangular subunits linked *via* two 'central' oximate O-atoms (O_{oxim}) and two 'peripheral' phenoxide O-atoms (O_{ph}), leading to a $[Mn^{III}_6(\mu_3\text{-}O)_2(\mu_3\text{-}ONR)_2(\mu\text{-}ONR)_4]^{8+}$ core. The bridging between neighbouring Mn ions within each triangle occurs through an NO oximate group, such that each Mn_2 pair forms a –Mn-N-O-Mn- moiety, and thus the Mn_3 triangle a $(\text{-Mn-O-N-})_3$ ring. In all complexes the coordination spheres of the Mn ions are completed by two terminal carboxylates (one on each triangle; except for complexes **1, 3-5** where the carboxylates are bridging in a $\eta^1{:}\eta^1{:}\mu$ fashion), a phenoxide O-atom, and by terminal alcohol solvent molecules and/or H_2O molecules. In complexes **23** and **24** the carboxylates are replaced by halides. All Mn ions are in the 3+ oxidation state, as confirmed by a combination of bond-length considerations, BVS calculations[12] and charge-balance. The Jahn-Teller axes all lie perpenidicular to the $[Mn_3O]^{7+}$ planes.

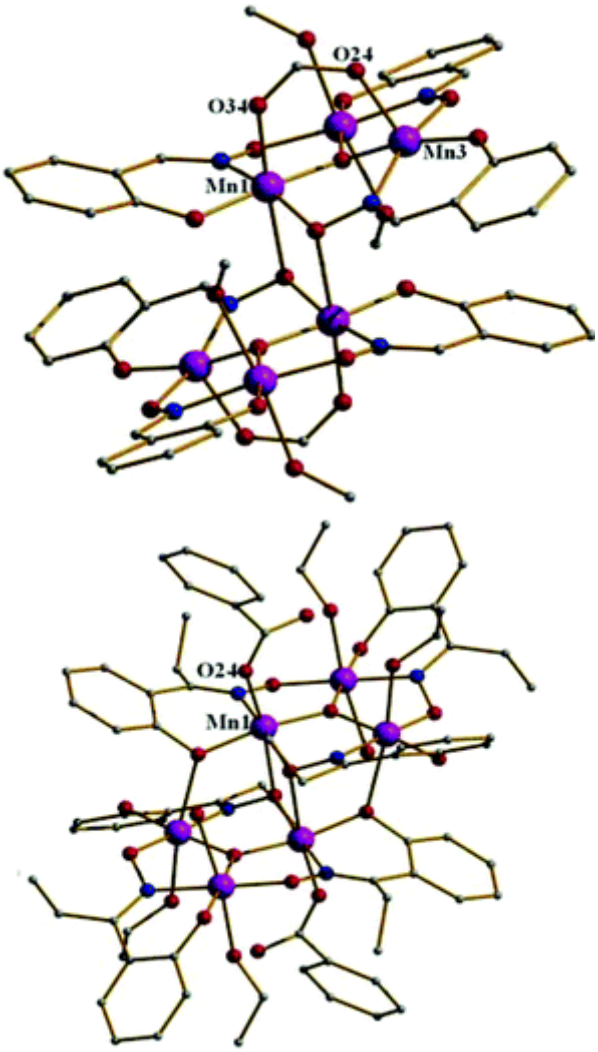

Figure 2. The molecular structures of **1** (top) and **14** (bottom) representing the two different structural types in the $[Mn_6]$ family. Colour code: Purple = Manganese, Red = Oxygen and Blue = Nitrogen.

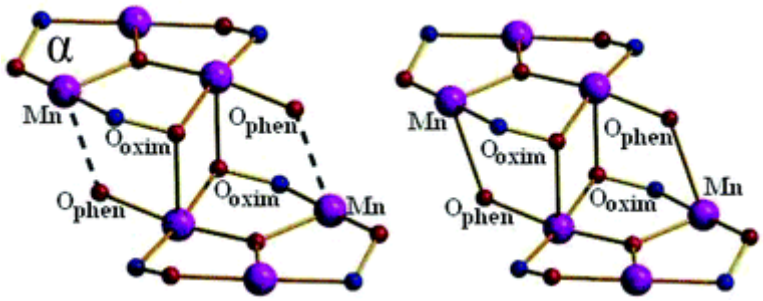

Figure 3. (left) The [Mn_6] core common to **1** and its analogues in which the carboxylate is bridging, showing the Mn-O_{phen} interaction involving a 5-coordinate Mn^{III} ion. (right) The [Mn_6] core common to **14** and its analogues in which the carboxylate or halide is terminally bonded. The Mn-N-O-Mn torsion angle is denoted α. Colour code as Figure. 2.

More detailed structural comparisons show that we can subdivide the 24-member family into two general types, [$Mn^{III}_6O_2$(R-sao)$_6$(X)$_2$(sol)$_4$] and [$Mn^{III}_6O_2$(R-sao)$_6$(X)$_2$(sol)$_{5,6}$], as a consequence of the distortion imparted on the core via the inclusion of increasingly bulky oxime ligands. This is illustrated in Figures. 2-3. Approximately half the family appears to possess two symmetry equivalent (s.e.) square-based pyramidal five-coordinate Mn^{III} ions (i.e Mn3 in Figure 2). On closer inspection it becomes clear that the Mn-O_{phen} distances vary greatly and range from a relatively short 2.374 Å in **17** to a rather long 3.524 **Å** in **1**. These Mn-O_{phen} interactions form two symmetry equivalent bridges (when sufficiently close) between the two [Mn_3O(R-sao)$_3$]$^+$ units which add to the two ever-present symmetry equivalent Mn-O_{oxim} bridges located at the "centre" of the [Mn_6] cores (Figure. 3). [Mn_6O_2(Et-sao)$_6$(O_2CPh^2OPh)$_2$(EtOH)$_4$] (**10**) differs to all others in this respect by possessing a genuine five coordinate Mn^{III} situated at the periphery of the [Mn_6] core and isolated from any $O_{phenolic}$ or O_{oxim} donor atoms. Table 1 shows that the Mn-O_{phen} distances decrease as the [Mn_6] cores become more structurally distorted (the oximes employed are bulkier).

The second major structural difference lies in the individual Mn-N-O-Mn torsion angles (α) within each [Mn_3O(R-sao)$_3$] unit which range from a minimum of 8.36 º (in **4**) to a maximum of 47.56 º (in **10**). As previously suggested,[11] it is clear that the individual Mn-N-O-Mn torsion angles are relatively small when the underivatised (or "planar") sao^{2-} ligands are employed in their construction (ranging from 8.36 to 29.83º), and become much larger (ranging from 16.76 to 47.56º) when the functionalised ("non-planar") Me-sao^{2-} and Et-sao^{2-} ligands are used. Finally, we can see that as the bulk of the oxime is increased and the triangles become more puckered it becomes impossible for the carboxylate ligand to bridge and it becomes terminally ligated instead of μ-bridging, with the vacated site occupied by an additional solvent molecule.

In short, as we replace sao^{2-} with its bulkier analogues R-sao^{2-} we force the carboxylate to bridge terminally, the Mn-O-N-Mn angle to be increasingly twisted (non-planar) and the Mn-O_{phen} distance to become shorter.

In general there are no significant intermolecular interactions observed between the individual [Mn_6] clusters containing bridging / terminal carboxylates (**1**-**22**). In some cases non-bonding solvent molecules of crystallisation (MeOH / EtOH) act as H-bonding connectors, linking the [Mn_6] moieties together via ROH…O_{phen} (R = Et, Me) interactions (e.g. as observed in **2**, **3**, **6** and **17**). The halogen containing complexes **23** and **24**, however, exhibit intramolecular interactions between the X^- ions (X = Br (**23**), I (**24**)) and nearby terminal EtOH molecules (Br1···H14(O8) = 2.459 Å, I1···H441(O44) = 2.687 Å). Intermolecular interactions observed in **23** are limited to H-bonding interactions between the terminal Br^- ligands and the aromatic protons belonging to the Et-sao^{2-} ligands of an adjacent [Mn_6] complex (Br1…H17(C17) = 2.859 Å). The crystal structure of **24** shows two types of close contact interactions. More specifically the I^- and oxygen atoms (of terminal EtOH ligands) of each [Mn_6] unit H-bond with the $–CH_3$ protons and aromatic C-$H_{aromatic}$ protons of nearest neighbour Me-sao^{2-} ligands, respectively (I1···H152(C15) = 3.178 Å, O38…H181(C18) = 2.713 Å).

Magnetic studies

Dc magnetic susceptibility studies were carried out on crystalline samples of **1**-**24** in the 5 - 300 K temperature range in a field of 0.1 T.[6,7] The magnetic susceptibility data obtained from each member were simulated using the MAGPACK[13] program employing the Hamiltonians in (1)-(3) (Scheme 1) to provide the isotropic parameters *S*, *J* and *g* summarised in Table 2. Figure. 4 shows the $\chi_M T$ vs. *T* data and, where possible, their associated simulations (solid lines). It is clear from Table 2 that for several complexes the experimental data do not allow for an undoubted determination of the ground spin state since there are many *S* states that are essentially degenerate; for example, see complexes **7**, **10**, **11**, **12** and **13**. However, we enter the values from the simulations for completeness. The magnetic susceptibility curves obtained illustrate how, despite their structural similarities, complexes **1**-**24** show dramatically different magnetic behaviour.

(1) $$\hat{\mathcal{H}} = -2J(\hat{S}_1\cdot\hat{S}_2 + \hat{S}_2\cdot\hat{S}_3 + \hat{S}_1\cdot\hat{S}_3 + \hat{S}_1\cdot\hat{S}_{2'} + \hat{S}_2\cdot\hat{S}_{3'} + \hat{S}_1\cdot\hat{S}_{3'} + \hat{S}_2\cdot\hat{S}_{3'} + \hat{S}_{2'}\cdot\hat{S}_3 + \hat{S}_2\cdot\hat{S}_{2'})$$

(2) $$\hat{\mathcal{H}} = -2J_1(\hat{S}_1\cdot\hat{S}_2 + \hat{S}_2\cdot\hat{S}_3 + \hat{S}_2\cdot\hat{S}_{3'} + \hat{S}_{2'}\cdot\hat{S}_3 + \hat{S}_1\cdot\hat{S}_{2'} + \hat{S}_2\cdot\hat{S}_{2'} + \hat{S}_{2'}\cdot\hat{S}_{3'}) - 2J_2(\hat{S}_1\cdot\hat{S}_3 + \hat{S}_1\cdot\hat{S}_{3'})$$

(3) $$\hat{\mathcal{H}} = -2J_1(\hat{S}_1\cdot\hat{S}_2 + \hat{S}_2\cdot\hat{S}_3 + \hat{S}_1\cdot\hat{S}_{2'} + \hat{S}_{2'}\cdot\hat{S}_{3'}) - 2J_2(\hat{S}_1\cdot\hat{S}_3 + \hat{S}_1\cdot\hat{S}_{3'}) - 2J_3(\hat{S}_2\cdot\hat{S}_{3'} + \hat{S}_2\cdot\hat{S}_{2'} + \hat{S}_{2'}\cdot\hat{S}_3)$$

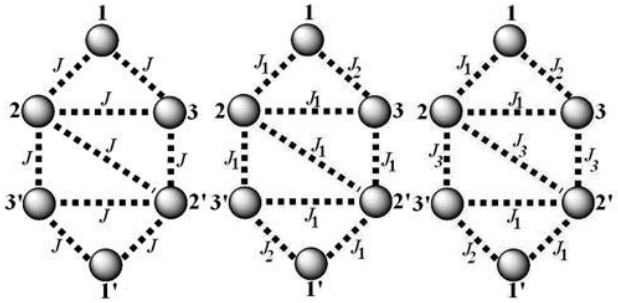

Scheme 1. Schematic detailing the 1, 2- and 3-*J* models employed to simulate the experimental data.

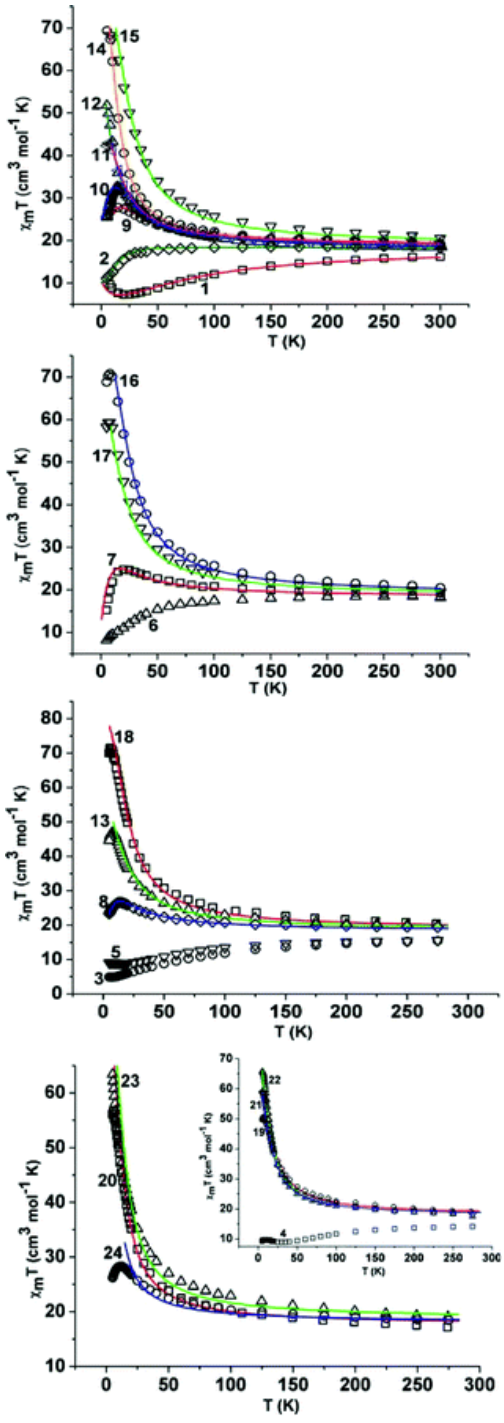

← ***Figure 4.*** Plots of $\chi_M T$ vs. T for complexes **1-24**. The solid lines represent simulations of the experimental data in the temperature range 300 – 5 K. For parameters see Table 2.

The $\chi_M T$ vs. T curves obtained for complexes **1-6** show dominant antiferromagnetic exchange with room temperature values ranging from 13.88 to 18.38 cm^3 mol^{-1} K. In each case $\chi_M T$ remains approximately constant before dropping more rapidly at temperatures below 100 K and reaching values of between 4.91 and 11.12 cm^3 mol^{-1} K. In the case of **1** a slight upturn in $\chi_M T$ was observed at 25 K reaching a maximum value of 9.71 cm^3 mol^{-1} K at 5 K.

Despite attempts to use the 1-*J* and 2-*J* models of Scheme 1, the data obtained for complex **1** could only be simulated with the 3-*J* model described by Eqn. (3), giving $S = 4$, $J_1 = 1.25$, $J_2 = -4.6$, $J_3 = -1.8$ cm^{-1} and $g = 1.99$. A 2-*J* model (Eqn. (2)) was employed to simulate the experimental data obtained from complex **2** to yield the parameters $S = 4$, $J_1 = +1.2$, $J_2 = -1.95$ cm^{-1}, $g = 2.01$. Despite much effort we were unable to successfully simulate the data for complexes **3-6**. The $\chi_M T$ vs. T curves obtained from complexes $[Mn_6O_2(Et\text{-}sao)_6(O_2CC_{12}H_{17})_2(EtOH)_4(H_2O)_2]$ (**7**) and $[Mn_6O_2(Et\text{-}sao)_6(O_2CC(CH_3)_3)_2(MeOH)_6]$ (**8**) appear very similar in line shape to those obtained from **1-6** with similar room temperature values of 18.54 and 19.41 cm^3 mol^{-1} K, respectively. In both cases $\chi_M T$ remains constant until a temperature of approximately 50 K where a gradual increase occurs before reaching maxima at 20 and 10 K and $\chi_M T$ values of 28.80 and 26.02 cm^3 mol^{-1} K, respectively. The value then drops sharply in both cases to 15.29 and 23.32 cm^3 mol^{-1} K at 5 K. Simulation of these data using the 2-*J* model (2) suggests ground spin states of $S = 5\pm1$ (**7**) and $S = 5$ (**8**) (Table 2) but with many (excited) states that are essentially degenerate.

Magnetic susceptibility studies on complexes **9-13** show room temperature $\chi_M T$ values in the 18.48 - 19.88 cm^3 mol^{-1} K range which gradually increase with decreasing temperature, reaching low temperature values of between 25.43 and 42.32 cm^3 mol^{-1} K. Such values lie between the two $S = 4$ (10 cm^3 mol^{-1} K) and $S = 12$ (78 cm^3 mol^{-1} K) extremes and suggest 'intermediate' ($4 < S < 12$) ground spin states, diagnostic of competing anti- and ferromagnetic exchange between the Mn^{III} ions. This is corroborated by the spin Hamiltonian parameters obtained from the simulation of the experimental data (see Table 2): a 2-*J* model was employed for complexes **9-13** affording $S = 6$, $g = 2.01$, $J_1 = 1.39$ and $J_2 = -1.92$ cm^{-1} (**9**); $S = 7\pm1$, $g = 1.97$, $J_1 = 1.76$ and $J_2 = -1.92$ cm^{-1} (**10**); and $S = 9\pm1$, $g = 1.98$, $J_1 = 1.39$ and $J_2 = -0.99$ cm^{-1} (**11**). The simulations for **12** and **13** give $S = 11\pm1$ ground states. Again it is clear that in each case the presence of weak exchange leads to a situation in which many S states are essentially degenerate making assignment of a ground state difficult and in some cases perhaps inappropriate.

The third type of susceptibility curve (complexes **14-24**) shows a constant increase in $\chi_M T$ with decreasing temperature indicative of ferromagnetic exchange between the Mn centres. The room temperature $\chi_M T$ values are all above 18.0 cm^3 mol^{-1} K and in each case increase gradually before rising more abruptly in the 75-100 K temperature region. The maximum $\chi_M T$ values range between 49.71 and 69.95 cm^3 mol^{-1} K. All exhibit $S = 12$ ground states with $S = 11$ excited states at energies of up to 9 cm^{-1} (Table 2) above the ground state. It should be noted that the $\chi_M T$ vs. T curve obtained for $[Mn_6O_2(Me\text{-}$

sao)$_6$(I)$_2$(EtOH)$_6$] (**24**) reaches a rather low maximum value 28.31 cm^3 mol^{-1} K suggestive of the presence of an "intermediate" spin ground state (Figure 4); however simulation of the data shows this not to be the case (S = 12, g = 2.00, J_1 = +0.95 and J_2 = +0.40, Table 2) - the lineshape and the low temperature downturn in $\chi_M T$ being attributed to the significant intermolecular interactions observed in its crystal structure (*vida supra*). The S = 12 ground states may be simply explained as a product of six ferromagnetically coupled Mn^{III} ions, while the S = 4 ground spin states may be rationalised as two antiferromagnetically coupled (S = 2) [Mn$^{III}_3$] triangles which are ferromagnetically coupled to one another.[6,7,11] Each Mn$\cdots$Mn pair is relatively weakly coupled with J values of < 2 cm^{-1} - in line with previously reported values for oxime-bridged Mn$^{III}\cdots$Mn^{III} complexes.[9] Many, indeed probably all, members of this large family exhibit non-isolated spin ground states,[11,14] the "nesting" of excited states on the ground state being a direct result of the weak magnetic coupling - resulting in the breakdown of the so-called "*giant spin*" model.[14] With this in mind and within the confines of our simplistic model, variable field and temperature dc magnetisation data were collected in the 0.5–7 T and 2-7 K field and temperature ranges. In each case we attempted to fit the data with an axial ZFS plus Zeeman Hamiltonian (4) by a method described recently by Piligkos in the whole field and temperature range,[15]

(4) $\mathcal{H} = D(\hat{S}_z^2 - S(S+1)/3) + \mu_B g H \hat{S}$

where D is the axial anisotropy, μ_B is the Bohr magneton, $\hat{S}_z$ is the easy-axis spin operator, and H is the applied field. The results are summarised in Table 2 with representative plots given in Figure. 5. Complexes **1**-**9** possess relatively low spin ground states (S = 4, 5 and 6) with D values ranging from -0.75 to -1.59 cm^{-1}, while the ferromagnetic complexes (**14**-**24**) in the lower half of Table 2 possess much smaller zfs parameters ranging from D = -0.34 cm^{-1} to -0.44 cm^{-1}.[6,7,11] A previously reported ligand field study on a sub-group of this [Mn$_6$] family revealed the differences in their ground state anisotropies stem from the difference in projection coefficients of the single ion aniostropy to spin states of different total spin quantum number (S) and not the geometrical distortions of the individual metal ions.16

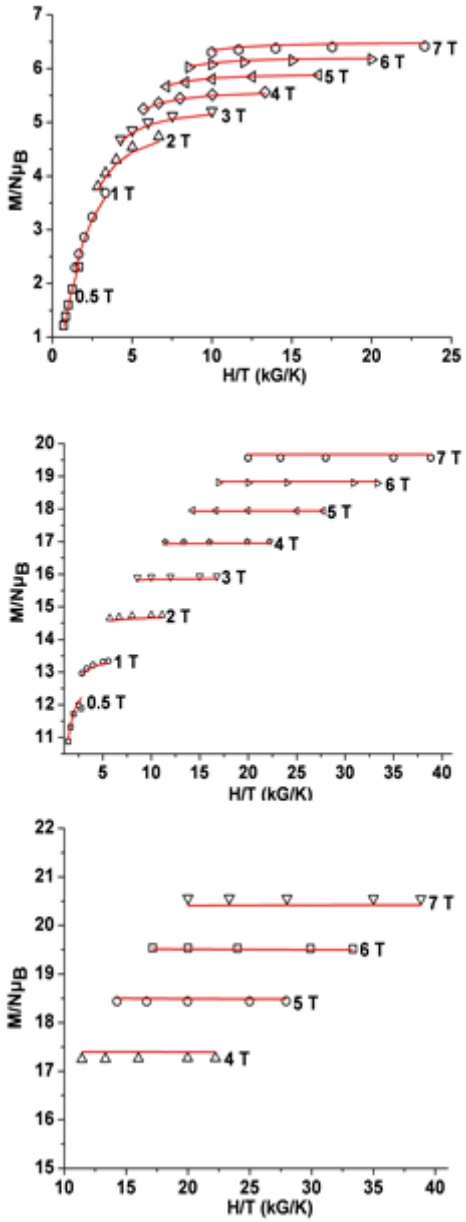

Figure 5. Plots of reduced magnetisation ($M/N\mu_B$) versus H/T for **4** (top), **14** (middle) and **15** (bottom) in the noted field ranges and the 2 – 6 K temperature range. The solid lines correspond to the fit of the data as documented in Table 2.

Each member of this family possesses a non-zero spin ground state ($4 \leq S \geq 12$) with sizeable zfs, both of which are prerequisites for single-molecule magnetism behaviour. In order to investigate this in more detail, ac magnetic susceptibility measurements were carried out on crystalline samples of **1**-**24** in the 2 – 10 K temperature range in a 3.5 G ac field oscillating at frequencies ranging from 50 to 1000 Hz. Fully visible out-of-phase (χ_M'') signals indicative of SMM behaviour (Figure. 6 shows those obtained for complex **14**) were observed for *all* family members except for $[Mn_6O_2(sao)_6$(keto-

acetate)$_2$(EtOH)$_2$(H$_2$O)$_2$] (**3**), [Mn$_6$O$_2$(Me-sao)$_6$(O$_2$C-th)$_2$(EtOH)$_4$(H$_2$O)$_2$] (**6**) and [Mn$_6$O$_2$(Me-sao)$_6$(I)$_2$(EtOH)$_6$] (**24**), in which only the tails and not the peaks of the signals were observed. The ac data obtained were combined with single-crystal dc relaxation measurements performed on a μ-SQUID[17] and fitted to the Arrhenius equation $\tau = \tau_o \exp(U_{eff}/(kT))$, where τ_o is the prexponential factor, τ is the relaxation time, U_{eff} is the barrier to the relaxation of the magnetisation and k is the Boltzmann constant, to give the effective barrier to magnetisation reorientation (U_{eff}) for each [Mn$_6$] complex. These data are summarised in Figure. 7 and Table 2 and span barrier heights of between ~24-86 K.

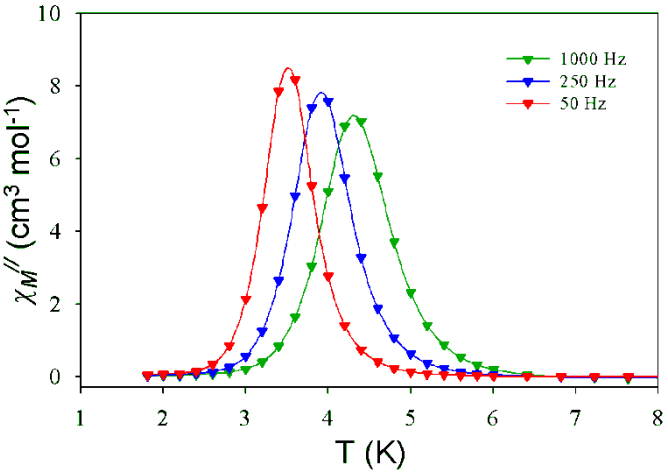

Figure 6. AC out-of-phase χ''_M vs. T plot obtained for complex **14** in an oscillating field of 3.5 Oe and frequencies of 50-1000 Hz.

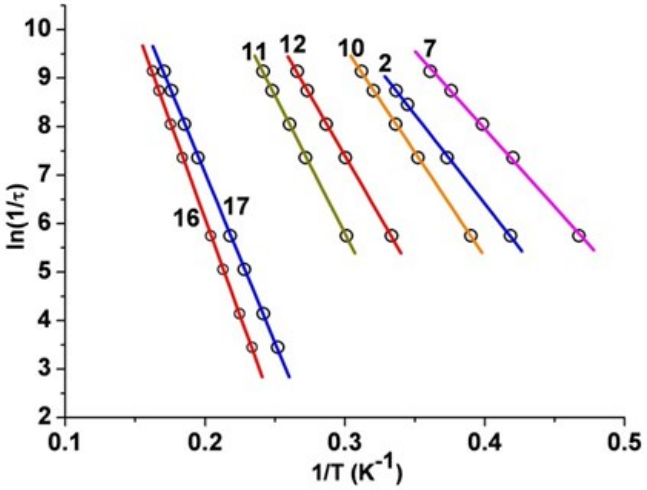

Figure 7. Plots of ln(1/ τ) vs. 1/T obtained from ac magnetic susceptibility data for a cross section of family members.

High Frequency Electron Paramagnetic Resonance Studies

High frequency EPR measurements were performed on single crystals of complex **2** (S = 4) and **15** (S = 12) to verify the ground state spin value and the zero field splitting (ZFS) parameters. Details of the experimental technique can be found elsewhere.[18,19] Figure. 8 displays easy-axis (*B*//*c*) temperature dependent spectra obtained for complex **15** at 331 GHz. With increasing temperature, several strong peaks labeled ***a***, ***b***, ***c***, ***d*** and ***e*** are observed within the field range of the magnet, corresponding to the following fine-structure transitions: m_S = -12 → -11, -11 → -10, -10 → -9, -9 → -8 and -8 → -7, respectively, where m_S represents the spin projection onto the easy axis of the crystal. Weaker satellite peaks seen as shoulders on the main peaks appear to be caused by a slight *D*-strain in the sample, i.e. a small fraction of molecules experiencing different microenvironments and, hence, different (lower) *D*-values.[20] Multi-frequency measurements enabled accurate determination of the following ZFS parameters for the majority species (strongest resonance peaks) associated with complex **15**: D = -0.360(5) cm^{-1}, B_4^0 = -5.7(5) × 10^{-6} cm^{-1} and g = 1.98(1) for this S = 12 complex.

The inset to Figure. 8 shows the easy-axis spectrum for complex **2** obtained at 285 GHz and 15 K. Several resonances are again observed, most of which can be assigned to fine-structure transitions within an S = 4 ground state, i.e. m_S = -4 → -3, -3 → -2, etc. However, attempts to fit the entire spectrum using a single-spin description were not entirely satisfactory. Nevertheless, through combined multi-frequency and temperature dependent measurements, we were able to ascertain that some of the peaks correspond to transitions within low-lying excited spin multiplets (labeled *ES* in the inset to Figure. 8).[21,22] The remaining peaks could then be fit to a S = 4 model, allowing us to determine approximate ZFS parameters associated with this multiplet: D = -1.27(2) cm^{-1} and B_4^0 = +1.3(3) × 10^{-4} cm^{-1}. The observation of excited state intensity in the spectrum of complex **2** is not surprising given the frustrated interactions within the triangular Mn_3 units.

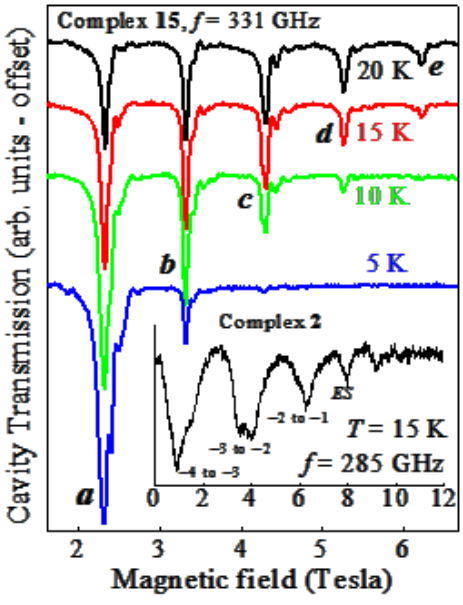

← ***Figure 8.*** Easy axis temperature dependence spectra for complex **15** at 331 GHz. The inset shows the easy axis spectrum for complex **2** at 285 GHz, 15 K.

The use of a giant spin description to fit the EPR spectra allows for direct comparisons with magnetic measurements. In particular, one can estimate the magnetisation reversal barriers for both complexes: 29.2 K for the low spin system (**2**) and 75 K for the high spin system (**15**), *i.e.* an increase by a factor of 2.56, which is in good agreement with the AC susceptibility measurements (an increase of 2.70).[21,22]

Discussion

Understanding the relationship between structure and magnetic behaviour in polymetallic cluster compounds is an extremely difficult task, and increasingly so as the nuclearity increases, since one must consider all contributions to the exchange, including, for example, the innocence or non-innocence of (terminal) co-ligands.[23] For the [Mn_6] family this means we must consider the combination of four different ligand types (oxime, phenoxide, oxide and carboxylate), their relative positions, the bond lengths and angles associated with each; and at least four different exchange interactions. A comprehensive *quantitative* analysis is thus rather difficult to achieve and will require theoretical input.[24] In earlier work we suggested that while clearly *all* magnetic pathways must play some role in determining the size and magnitude of the Mn···Mn exchange, the dominant factor was the twisting of the Mn-O-N-Mn moiety as induced by the distortion imposed on the molecule by bulkier oximes (R-sao^{2-}).[11] In order to shed further light on this we have examined all of the structural parameters in the magnetic cores of complexes **1**-**24**. In particular we have examined the relationship between the observed *J*-value for a particular Mn···Mn exchange and (a) the out-of-plane shift of the central oxide - previous studies on analogous trinuclear systems have suggested an increasingly ferromagnetic interaction as this distance increases;[25] (b) the Mn-(μ_3-O)-Mn angle - experimental studies of [$Mn^{III}_3O(O_2CR)_6L_3$]$^+$ species suggest a switch from antiferromagnetic to ferromagnetic at angles below ~120º;[26] (c) the Mn^{III}-O^{2-} distances; (d) the Mn-N-O-Mn distances; (e) the Mn-N-O-Mn torsion angles, α. An examination of the data of Tables 1 and 2 allows us to make some general conclusions:

i) In all cases the exchange *between* the [Mn_3] triangles appears to be ferromagnetic.

ii) The exchange between Mn_2 pairs is dominated by the Mn-O-N-Mn torsion angles; the larger the torsion angle, the more ferromagnetic the pairwise interaction; the smaller the Mn-N-O-Mn torsion angle the more antiferromagnetic the pairwise interaction.

iii) Above a torsion angle of approximately 31^o the exchange appears to switch from antiferromagnetic to ferromagnetic, i.e. if α > ~31^o, then J > 0 (F); if α < 31^o then J < 0 (AF). When a [Mn_3] triangle contains torsion angles that are both above and below this value the data can only be simulated using both F and AF exchange.

iv) It is the individual torsion angles between neighbouring Mn ions that dictates the behaviour of the

complex, and not the average torsion angle. For example, complex **2** has α_v= 32.5° but an S = 4 ground state, complex **14** has α_v= 36.5° and an S = 12 ground state, and complex **11** has α_v= 37.4° and an $S \approx 9$ ground state.

v) The presence of the carboxylate in either coordinating mode (μ or terminally bonded) appears to have little effect on the sign of J. This is exemplified by complexes **1** and **6**, both of which display S = 4 ground states despite the fact that the former contains a bridging carboxylate and the latter a terminal carboxylate. The synthesis of the $[Mn^{III}_6O_2(Et\text{-}sao)_6(Br)_2(EtOH)_6]$ (**23**) and $[Mn^{III}_6O_2(Me\text{-}sao)_6(I)_2(EtOH)_6]$ (**24**) derivatives shows that we are able to replace the peripheral $^{-}O_2CR$ carboxylate groups with halides while keeping the $[Mn_6]$ core intact; the magnetic properties of these complexes appear identical.[27]

vi) If each Mn_2 exchange is ferromagnetic (i.e. an S = 12 complex), the larger the Mn-N-O-Mn torsion angle (α), the larger the barrier to magnetisation relaxation (U_{eff}). For example, comparing complexes **14** and **16** (Table 2) with J = +0.93 cm^{-1} and J= +1.60 cm^{-1}, respectively, the U_{eff} values are 53.1 K and 79.9 K. This presumably arises because an increase in torsion angle leads to an increase in $|J|$ which results in a more isolated ground state, and a reduction in tunneling.[14] This is reflected in the simulation of the susceptibility data. For example in complex **14** (S = 12) where J= +0.93 cm^{-1}, the first excited state of S = 11 is located only 5 cm^{-1} above the ground-state, whereas in complex **15** (S = 12) where J= +1.63 cm^{-1} the first excited state of S = 11 is located 9 cm^{-1} above the ground-state, *i.e.* twice as high. However, given the complicated nature of the magnetic relaxation in such species,[14] one has to treat this statement as somewhat speculative.

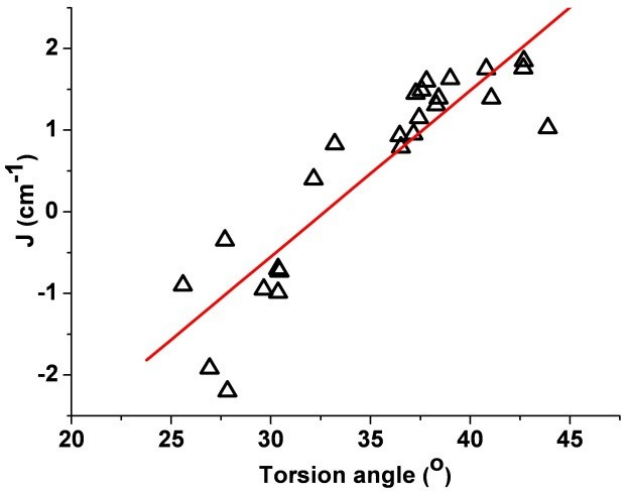

Figure 9. Plot of best fit parameter J vs. Mn-N-O-Mn torsion angle (°) taken from all members of the $[Mn_6]$ family. Note: As necessary due the confines of this study, the mean average torsion angles were used to construct this *qualitative* plot.

In summary, an examination of Tables 1 and 2 suggests no *obvious* correlation between *J* and any of (a)-(d), but there does appear to be a correlation between the magnitude of the exchange and the Mn-N-O-Mn torsion angle - the larger the torsion angle the more ferromagnetic the pairwise exchange. This has also been suggested in recent DFT calculations on analogous oxime-bridged [Mn_3] triangles.[6d,28] Figure. 9 shows a plot of torsion angle (α) versus *J*-value for the [Mn_6] family; a linear fit suggesting $J = 0$ at a torsion angle value of approximately 31° - in good agreement with previous predictions.[11] It is important to emphasise of course that this is purely *qualitative* in nature, since in each case we simulated the experimental susceptibility data using the most simple model available, for example, for complex **15** we employed a 1-*J* model even though four different exchange interactions are present. Indeed it is clear that these are very complicated molecules. It is likely that most, if not all, possess excited states nested upon the ground state rendering the analysis and interpretation of the data within the giant-spin model somewhat difficult and qualitative in nature, albeit with clearly defined trends. We also point out, as we have done on several occasions, that the above correlation is (unfortunately) valid *only* for this family of [Mn_6] molecules (and the structurally analogous "half" [Mn_3] complexes)[29] and it is unlikely that it can be extended to other systems. Those investigating the exchange within similar $[Mn_3O]^{n+}$ triangles,[4,25] even if they are oxime-based, should thus bear this caveat in mind. In our opinion it is unwise to assume that the same "twisting" rules we introduced to exploit and explain the behaviour of **1**-**24** can applied to molecules that, despite some obvious similarities, clearly have different strutural architectures.

Conclusions

We have synthesised and characterised twenty four members of a hexametallic [Mn_6] family of Single-Molecule Magnets. Each member possesses a common $[Mn_6O_2(R\text{-}sao)_6]^{2+}$ core comprising two linked $[Mn_3O(R\text{-}sao)_3]^{+}$ triangles. The type of magnetic exchange within the molecule can be controlled using targeted structural distortion of the core. By employing "planar" non-derivatised oximes ($saoH_2$) the molecules are "unpuckered", the dominant intra-triangle exchange is antiferromagnetic and the molecules have low spin ($S = 4$ ground states). By derivatising the oxime carbon atom to contain bulkier substituents, the [Mn_6] molecules become increasingly puckered as evidenced by large increases in the Mn-N-O-Mn torsion angles. The result is that pairwise exchange becomes increasingly ferromagnetic, resulting in ferromagnetic molecules with $S = 12$ spin ground states. Qualitatively, the "switch" from antiferromagnetic to ferromagnetic comes at an Mn-N-O-Mn angle above approximately 31°. DFT calculations on the whole family are currently underway and will reported separately.[28] More recent developments have also focused on synthesizing the analogous 'half' molecules, *i.e.* the species $[Mn_3O(R\text{-}sao)_3(O_2CR')_1(sol)_x]$ (R = H, Me, Et, Ph; R′ = CH_3, $Ph(Cl)_2$, $Ph(CF_3)_2$ etc; sol = py, H_2O, EtOH),[29] in order to shed yet further light on this intriguing family of nanomagnets.

Experimental

All manipulations were performed under aerobic conditions, using materials as received. CAUTION! Although no problems were encountered in this work, care should be taken when using the potentially explosive perchlorate anion.

The syntheses, structures and magnetic properties of complexes **1**, **2**, **6**, **7**, **9-12**, **14-20**, **23** and **24** have already been communicated or reported.[5a, 5b, 7a, 7b, 27, 30] Compounds **3-5**, **8**, **13**, **21** and **22** are reported here for the first time. General synthetic strategy applicable to all twenty four compounds:

Method A. To pale pink solutions of $Mn(ClO_4)_2 \cdot 6H_2O$ in MeOH (EtOH or MeCN) were added equivalent amounts of the derivatized oximes, the corresponding carboxylic acid and CH_3ONa (or NEt_4OH). The solutions were left stirring for ~30 min, filtered and then left to slowly evaporate. In each case suitable crystals grew after a period of 3-5 days.

Method B. The sodium salt of the corresponding carboxylic acid was treated with equivalent amounts of $Mn(ClO_4)_2 \cdot 6H_2O$, the derivitized oximes and CH_3ONa (or NEt_4OH) in MeOH (or EtOH). Single crystals were grown upon slow evaporation.

Method C (for complexes **23** and **24**). The $Mn(ClO_4)_2 \cdot 6H_2O$ metal source was replaced with $Mn^{II}X_2.4H_2O$ (X = Br^- (**23**), I^- (**24**) and reacted with one equivalent of R-saoH_2 (R = Et (**23**), Me (**24**)) and $NEt_4(OH)$ base in EtOH. Single crystals were obtained upon slow evaporation of these dark green / black solutions. For all 24 compounds the yields vary from minimum of 30% to a maximum of 50%.

Elemental Anal. calcd (found) for dried **3** solvent free: C 47.75 (47.08), H 4.67 (4.26), N 4.64 (4.46). **4**: C 48.61 (48.49), H 3.85 (4.03), N 11.02 (10.74). **5**: C 46.67 (46.85), H 4.90 (4.33), N 5.10 (4.96). **8**: C 48.45 (48.26), H 5.58 (5.04), N 4.84 (5.03). **13**: C 45.41 (45.64), H 5.39 (4.87), N 4.89 (4.89). **21**: C 50.91 (50.67), H 5.13 (5.09), N 4.45 (4.12). **22**: C 44.20 (43.95), H 4.09 (4.02), N 4.55 (4.83).

Variable temperature, solid-state direct current (dc) and alternating current (ac) magnetic susceptibility data down to 1.8 K were collected on a Quantum Design MPMS-XL SQUID magnetometer equipped with a 7 T dc magnet. Diamagnetic corrections were applied to the observed paramagnetic susceptibilities using Pascal's constants. Magnetic studies below 1.8 K were carried out on single crystals using a micro-SQUID apparatus operating down to 40 mK,[17] and using a magnetometer consisting of a micro-Hall bar.[21]

Diffraction data were collected at 150 K on a Bruker Smart Apex CCDC diffractometer, equipped with an Oxford Cryosystems LT device, using Mo radiation.[31] See CIF files for full details and Table SI1 in the ESI. CCDC-706507 (**3**), CCDC-706508 (**4**), CCDC-706509 (**5**), CCDC-706510 (**8**), CCDC-706504 (**13**), CCDC-706505 (**21**) and CCDC-706506 (**22**) contain the supplementary crystallographic data for this paper. These data can be obtained free of charge from CCDC via www.ccdc.cam.ac.uk/data_request/cif.

Tables

Complex	Mn-(μ_3-O) distance/Å	Mn-(μ_3-O)-Mn angles/°	Mn_{3plane}-(μ_3-O)/Å	Mn-O_{phen}/Å	Mn-O_2CR'/Hal^- distance/Å
	Mn1-O, Mn2-O, Mn3-O	Mn1-2, Mn2-3, Mn1-3			
$[Mn_6O_2(sao)_6(O_2CH)_2(MeOH)_4]$ (**1**)	1.872(2), 1.879(2), 1.857(2)	119.36(8), 121.42(8), 114.90(8)	0.226	3.524	2.138(2), 2.112(2)
$[Mn_6O_2(Me\text{-}sao)_6(O_2CCPh_3)_2(EtOH)_4]$ (**2**)	1.874(2), 1.898(2), 1.864(2)	119.76(9), 119.55(9), 120.18(9)	0.078	2.384	2.062(2)
$[Mn_6O_2(sao)_6(ketoacetate)_2(EtOH)_2(H_2O)_2]$ (**3**)	1.863(2), 1.869(2), 1.877(2)	115.33(8), 120.75(8), 120.16(8)	0.211	3.582	2.096(2), 2.129(2)
$[Mn_6O_2(sao)_6(O_2CPh)_2(MeCN)_2(H_2O)_2]$ (**4**)	1.868(2), 1.873(2), 1.872(2)	115.28(9), 120.50(9), 121.27(9)	0.186	3.271	2.104(2), 2.148(2)
$[Mn_6O_2(sao)_6(1\text{-}Me\text{-}cyclohex)_2(MeOH)_4]$ (**5**)[a]	1.869(2), 1.867(2), 1.877(2)	122.04(11), 115.71(11), 119.37(11)	0.184	3.348	2.127(2), 2.116(2)
	1.878(2), 1.850(2), 1.875(2)	121.50(11), 115.82(10), 119.84(10)	0.182	3.606	2.099(2), 2.106(2)
$[Mn_6O_2(Me\text{-}sao)_6(O_2C\text{-}th)_2(EtOH)_4(H_2O)_2]$ (**6**)	1.882(2), 1.863(2), 1.880(2)	119.43(10), 121.73(11), 118.79(11)	0.025	2.619	2.135(2)
$[Mn_6O_2(Et\text{-}sao)_6(O_2CC_{12}H_{17})_2(EtOH)_4(H_2O)_2]$ (**7**)	1.875(2), 1.884(2), 1.887(2)	120.22(6), 117.50(5), 121.45(5)	0.100	2.519	2.114(2)
$[Mn_6O_2(Et\text{-}sao)_6(O_2CC(CH_3)_3)_2(MeOH)_6]$ (**8**)	1.872(4), 1.883(3), 1.892(4)	119.93(19), 118.17(18), 120.95(18)	0.107	2.478	2.115(4)
$[Mn_6O_2(Et\text{-}sao)_6(O_2CC(CH_3)_3)_2(EtOH)_5]$ (**9**)[b]	1.891(3), 1.885(3), 1.876(3)	119.09(13), 119.93(13), 120.55(13)	0.072	2.458	2.104(3)
	1.883(3), 1.864(3), 1.892(3)	120.15(14), 120.28(13), 118.63(13)	0.105	2.388	2.131(3)
$[Mn_6O_2(Et\text{-}sao)_6(O_2CPh^2OPh)_2(EtOH)_4]$ (**10**)	1.881(4), 1.887(4), 1.853(4)	119.10(2), 119.60(2), 121.00(2)	0.057	2.379	2.098(5)
$[Mn_6O_2(Et\text{-}sao)_6(O_2CPh^4OPh)_2(EtOH)_4(H_2O)_2]$ (**11**)	1.875(1), 1.879(1), 1.888(1)	120.56(5), 118.64(5), 120.53(5)	0.057	2.417	2.118(2)
$[Mn_6O_2(Me\text{-}sao)_6(O_2CPhBr)_2(EtOH)_6]$ (**12**)	1.941(2), 1.900(2), 1.837(2)	125.47(12), 116.36(12), 117.63(12)	0.080	2.491	2.086(2)
$[Mn_6O_2(Me\text{-}sao)_6(O_2CC(CH_3)_3)_2(MeOH)_6]$ (**13**)	1.874(2), 1.878(2), 1.886(2)	120.22(10), 118.67(9), 120.96(9)	0.042	2.411	2.072(2)
$[Mn_6O_2(Et\text{-}sao)_6(O_2CPh)_2(EtOH)_4(H_2O)_2]$	1.878(2),	119.99(8), 118.21(8),	0.090	2.488	2.118(2)

Complex	Mn-(μ_3-O) distance/Å	Mn-(μ_3-O)-Mn angles/°			
	Mn1-O, Mn2-O, Mn3-O	Mn1-2, Mn2-3, Mn1-3	Mn_{3plane}-(μ_3-O)/Å	Mn-O_{phen}/Å	Mn-O_2CR'/Hal^- distance/Å
(**14**)	1.884(2), 1.888(2)	121.12(8)			
$[Mn_6O_2(Et\text{-}sao)_6(O_2CPh(Me)_2)_2(EtOH)_6]$ (**15**)	1.890(3), 1.889(3), 1.877(2)	118.48(13), 121.31(13), 120.11(13)	0.034	2.480	2.131(3)
$[Mn_6O_2(Et\text{-}sao)_6(O_2C_{11}H_{15})_2(EtOH)_6]$ (**16**)	1.881(2), 1.889(2), 1.886(2)	121.04(7), 118.72(7), 120.01(7)	0.053	2.438	2.106(2)
$[Mn_6O_2(Et\text{-}sao)_6(O_2CPh(Me))_2(EtOH)_4(H_2O)_2]$ (**17**)	1.879(2), 1.894(2), 1.878(2)	120.39(7), 118.94(7), 120.12(7)	0.081	2.374	2.126(2)
$[Mn_6O_2(Et\text{-}sao)_6(O_2C\text{-}Napth)_2(EtOH)_4(H_2O)_2]$ (**18**)	1.888(2), 1.870(2), 1.886(2)	121.35(11), 119.09(11), 118.67(11)	0.103	2.509	2.103(2)
$[Mn_6O_2(Et\text{-}sao)_6(O_2C\text{-}Anthra)_2(EtOH)_4(H_2O)_2]$ (**19**)	1.875(4), 1.886(4), 1.886(4)	120.9(2), 118.4(2), 120.0(2)	0.096	2.522	2.149(4)
$[Mn_6O_2(Et\text{-}sao)_6(O_2CPh(C{\equiv}CH)_2(EtOH)_4(H_2O)_2]$ (**20**)	1.876(2), 1.878(2), 1.881(2)	121.23(9), 117.87(9), 120.44(9)	0.074	2.482	2.116(2)
$[Mn_6O_2(Me\text{-}sao)_6(O_2CPh(C{\equiv}CH))_2(EtOH)_6]$ (**21**)	1.871(2), 1.892(2), 1.885(1)	119.91(9), 117.89(9), 121.52(10)	0.090	2.441	2.129(5)
$[Mn_6O_2(Me\text{-}sao)_6(O_2CPh(Cl)_2)_2(MeOH)_6]$ (**22**)	1.874(2), 1.883(2), 1.884(2)	120.19(10),118.38(9), 120.92(10)	0.081	2.447	2.114(2)
$[Mn_6O_2(Et\text{-}sao)_6(Br)_2(EtOH)_6]$ (**23**)	1.882(2), 1.888(2), 1.875(2)	118.85(11), 120.75(11), 120.38(11)	0.014	2.429	2.688(7)
$[Mn_6O_2(Me\text{-}sao)_6(I)_2(EtOH)_6]$ (**24**)	1.873(2), 1.883(2), 1.887(2)	120.03(9), 119.08(9), 120.06(9)	0.099	2.513	2.918(5)

a Two Mn_6 complexes in the asymmetric unit, therefore two sets of data documented.*b* Complex 9 has no centre of symmetry.

Table 1. Selected interatomic distances (Å) and angles (º) for complexes **1**-**24.**

Cmpl.	Crystal sys.	Sp. Grp.	α/°	J/cm^{-1}	S[b]	1$^{st}_{exc.}$ st./cm^{-1}[b]	g[c]	D/cm^{-1}[d]	τ_0/s[e]	U_{eff}/K[f]
			Mn1-2, Mn2-3, Mn1-3	J_1, J_2,J_3[a]						
(**1**)	Triclinic	*P*-1	25.57, 10.42, 18.01	+1.25, −4.6,−1.8	4	3(8)	1.99	−1.39	2.0×10^{-8}	28.0
(**2**)	Monoclinic	*C*2/*c*	25.50, 42.44, 29.74	+1.2, −1.95	4	5(10.5)	2.01	n.a.	6.8×10^{-10}	31.7
(**3**)	Triclinic	*P*-1	19.06, 18.89, 11.92	n.a.	4	n.a.	n.a.	n.a.	n.a.	n.a.
(**4**)	Triclinic	*P*-1	28.18, 16.18, 8.36	n.a.	4	n.a.	2.02	-1.59	6.57×10^{-8}	23.8
(**5**)	Triclinic	*P*-1	9.66, 29.83, 15.60	n.a.	4	n.a.	n.a	-1.18	1.70×10^{-8}	28.8
			13.53, 23.80, 37.33							
(**6**)	Triclinic	*P*-1	27.40, 31.10, 36.35	n.a.	n.a.	n.a.	n.a.	n.a.	n.a	n.a.
(**7**)	Triclinic	*P*-1	27.83, 40.07, 41.46	+1.55, −2.20	5 ± 1	4(0.01)	1.98	n.a.	9.3×10^{-10}	31.2
(**8**)	Triclinic	*P*-1	26.93, 34.45, 40.70	+1.49, −1.92	5	4(0.5)	2.01	n.a.	4.52×10^{-11}	59.2
(**9**)	Triclinic	*P*-1	36.92, 23.27, 42.12	+1.39, −1.92	6	7(0.5)	2.01	-0.75	3.0×10^{-8}	30.0
			32.33, 16.76, 42.24							
(**10**)	Monoclinic	*I*2/*a*	47.56, 31.76, 23.75	+1.76, −1.92	7 ± 1	6(0.1)	1.97	-0.39	1.5×10^{-10}	43.2
(**11**)	Triclinic	*P*-1	30.36, 38.38, 43.71	+1.39, −0.99	9 ± 1	8(0.03)	1.98	-0.37	1.2×10^{-10}	56.9
(**12**)	Triclinic	*P*-1	30.43, 42.94, 31.91	+1.15, −0.73	11 ± 1	12(0.2)	1.98	-0.50	1.7×10^{-10}	50.2
(**13**)	Triclinic	*P*-1	29.64, 38.51, 44.47	+1.65, −0.95	11 ± 1	12(0.02)	2.02	n.a	3.58×10^{-10}	57.6
(**14**)	Triclinic	*P*-1	31.26, 38.20, 39.92	+0.93	12	11(5)	1.99	-0.43	8.0×10^{-10}	53.1
(**15**)	Monoclinic	$P2_1/n$	39.10, 43.04, 34.86	+1.63	12	11(9)	1.99	-0.43	2×10^{-10}	86.4
(**16**)	Triclinic	*P*-1	42.61, 36.73, 34.07	+1.60	12	11(7.6)	1.99	-0.43	2.5×10^{-10}	79.9
(**17**)	Triclinic	*P*-1	47.16, 38.19, 30.37	+1.85, −0.70	12	11(1.4)	1.97	-0.44	7.5×10^{-10}	69.9
(**18**)	Monoclinic	$P2_1/c$	41.09, 33.28, 40.50	+1.31	12	11(6.23)	2.03	-0.34	4.33×10^{-10}	60.1
(**19**)	Triclinic	*P*-1	42.32, 39.28, 25.60	+1.75, −0.90	12	11(0.79)	2.00	-0.44	3.99×10^{-10}	60.1
(**20**)	Triclinic	*P*-1	38.85, 38.67, 32.06	+0.79	12	11(3.75)	1.97	n.a.	6.23×10^{-11}	66.8
(**21**)	Triclinic	*P*-1	43.61, 33.72, 29.53	+1.57, −0.70	12	11(0.91)	1.98	n.a.	4.37 ×	60.3

Cmpl.	Crystal sys.	Sp. Grp.	α/°	J/cm^{-1}	S[b]	1st exc. st./cm^{-1}[b]	g[c]	D/cm^{-1}[d]	τ_0/s[e]	U_{eff}/K[f]
			Mn1-2, Mn2-3, Mn1-3	J_1, J_2,J_3[a]					10^{-10}	
(**22**)	Triclinic	P-1	43.24, 27.61, 30.94	+1.45, −0.35	12	11(2.78)	1.98	-0.39	1.55 × 10^{-10}	48.5
(**23**)	Monoclinic	$P2_1/c$	33.40, 43.89, 33.00	+1.03, +0.83	12	11(3.99)	2.03	-0.36	5.45 × 10^{-10}	54.1
(**24**)	Monoclinic	$P2_1/c$	33.01, 31.28, 37.16	+0.95, +0.40	12	11(2.05)	2.00	-0.36	n.a.	n.a.

a Calculated from dc susceptibility studies.*b* Calculated from both dc susceptibility and magnetization measurements. The latter were collected in the field and temperature ranges 0–7 T and 2–7 K. In each case the data were fit by a matrix-diagonalization method to a model that assumes only the ground state is populated, includes axial zero-field splitting ($D\hat{S}_z^2$), and carries out a full powder average. The corresponding Hamiltonian is $H = D(\hat{S}_z^2 - S(S+1)/3) + \mu_B g H \hat{S}$ where D is the axial anisotropy, μ_B is the Bohr magneton, $\hat{S}_z$ is the easy-axis spin operator, and H is the applied field (see ref. 15).*c* Calculated from dc susceptibility measurements.*d* Calculated from magnetization measurements.*e* Calculated from dc susceptibility data and/or single-crystal relaxation measurements performed on a micro-SQUID; n.a. = not available.*f* Calculated from dc susceptibility data and/or single-crystal relaxation measurements performed on a micro-SQUID; n.a. = not available.

Table 2. Magnetostructural parameters for complexes **1**-**24**; Mn-N-O-Mn torsion angles *vs.* *J* and *S*.

Notes and references

‡Reaction of a simple Mn^{II} salt (e.g. $Mn^{II}(ClO_4)_2 \cdot 6H_2O$, $MnBr_2$, $MnCl_2 \cdot 4H_2O$ *etc*) with the (derivatised) salicyaldoxime ligand R-saoH_2 (R = H, Me, Et) in alcohol (ROH, R = Me, Et) in the presence of a carboxylic acid (or the corresponding sodium salt) and a suitable base (NaOMe, NH_4OH or NEt_3) affords hexametallic complexes of general formula $[Mn^{III}_6O_2(R\text{-sao})_6(X)_2(sol)_{4-6}]$ (R = H, Me, Et; X = carboxylate or halide ; sol = MeOH, EtOH H_2O) in excellent yields in 2–3 days.

[1] See for example (a) D. Gatteschi and R. Sessoli, *Angew. Chem., Int. Ed.*, 2003, **42**, 268; (b) M. Affronte, S. Carretta, G. A. Timco and R. E. P. Winpenny, *Chem. Commun.*, 2007, 1789; (c) J. Lehmann, A. Gaita-Arino, E. Coronado and D. Loss, *Nature Nanotech*., 2007, **2**, 312; (d) L. Bogani and W.Wernsdorfer, *Nature Mater.*, 2008, **7**, 179; (e) D. Gatteschi, R. Sessoli and J. Villain, *Molecular Nanomagnets*, Oxford University Press, 2006 and references therein.

[2] See for example (a) R. Sessoli, D. Gatteschi, A. Caneschi and M. A. Novak, *Nature*, 1993, **365**, 141; (b) M. N. Leuenberger and D. Loss, *Nature*, 2001, **410**, 789; (c) M. Evangelisti, F. Luis, L. J. de Jongh and M. Affronte, *J. Mater. Chem.*, 2006, **16**, 2534.

[3] (a) R. E. P. Winpenny, *Dalton Trans*., 2002, 1; (b) G. Aromí and E. K. Brechin, *Struct. Bond.,* 2006, **122**, 1, and references therein.

[4] See for example (a) C. J. Milios, T. C. Stamatatos and S. P. Perlepes, *Polyhedon,* 2006, **35**, 134-194; (b) A. G. Smith, P. A. Tasker and D. J. White, *Coord. Chem. Rev*. 2003, **241**, 61; (c) M. Viciano-Chumillas, S. Tanase, I. Mutikainen, U. Turpeinen, L. J. de Jongh and J. Reedijk, *Inorg. Chem*., 2008, 47, 5919; (d) S. Khanra, K. Kuepper, T. Weyhermüller, M. Prinz, M. Raekers, S. Voget, A. V. Postnikov, F. M. F. de Groot, S. J. George, M. Coldea, M. Neumann and P. Chaudhuri, *Inorg. Chem*., 2008, **47**, 4605; (e) C.-I.Yang, W. Wernsdorfer, G.-H.Lee, H.-L.Tsai, *J. Am. Chem. Soc*.,2007, **129**, 456.

[5] (a) C. J. Milios, A. Vinslava, P. A. Wood, S. Parsons, W. Wernsdorfer, G. Christou, S. P. Perlepes and E. K. Brechin. *J. Am. Chem. Soc*., 2007, **129**, 8; (b) C. J. Milios, A. Vinslava, W. Wernsdorfer, S. Moggash, S. Parsons, S. P. Perlepes, G. Christou and E. K. Brechin, *J. Am. Chem. Soc*., 2007, **129**, 2754. For other examples of structural distortion, see for example: (c) S. Accorsi, A.-L. Barra, A. Caneschi, G. Chastanet, A. Cornia, A. C. Fabretti, D. Gatteschi, C. Mortalo, E. Olivieri, F. Parenti, P. Rosa, R. Sessoli, L. Sorace, W. Wernsdorfer and L. Zobbi, *J. Am. Chem. Soc*., 2006, **128**, 4742; (d) D. Li, R. Clérac, G. Wang, G. T. Yee and S. M. Holmes, *Eur. J. Inorg. Chem*., 2007, 1341; (e) T. C. Stamatatos, K. A. Abboud, W Wernsdorfer and G. Christou, *Angew. Chem. Int. Ed*., 2007, **46**, 884; (f) A. M. Ako, V. Mereacre, R. Clérac, W. Wernsdorfer, I.J. Hewitt, C. E. Anson and A. K. Powell, *Chem. Commun.*, 2009, DOI: 10.1039/b814614d.

[6] (a) T. C. Stamatatos, D. Foguet-Albiol, C. C. Stoumpos, C. P. Raptopoulou, A. Terzis, W. Wernsdorfer, S. P. Perlepes and G. Christou, *J. Am. Chem. Soc.,* 2005, **127**, 15380; (b) C. J. Milios, A. G. Whittaker and E. K. Brechin, *Polyhedron*, 2007, 26, 1927; (c) C. J. Milios, P. A. Wood, S. Parsons, D. Foguet-Albiol, C. Lampropoulos, G. Christou, S. P. Perlepes and E. K. Brechin, *Inorg. Chim. Acta*, 2007, **360**, 3932; (d) J. Cano, T. Cauchy, E. Ruiz, C. J. Milios, C. C. Stoumpos, T. C. Stamatatos, S. P. Perlepes, G. Christou and E. K. Brechin, *Dalton Trans*., 2008, 234.

[7] (a) C. J. Milios, A. Vinslava, W. Wernsdorfer, A. Prescimone, P. A. Wood, S. Parsons, S. P. Perlepes, G. Christou and E. K. Brechin, *J. Am. Chem. Soc*., 2007, **129**, 6547; (b) C. J. Milios, R. Inglis, A. Vinslava, R. Baghi, W. Wernsdorfer, S. Parsons, S. P. Perlepes, G. Christou and E. K. Brechin., *J. Am. Chem. Soc*., 2007, **129**, 12505.

[8] (a) C. J. Milios, PhD Thesis, University of Patras, Greece, 2004; (b) C. J. Milios, C. P. Raptopoulou, A. Terzis, F. Lloret, R. Vicente, S. P. Perlepes and A. Escuer, *Angew. Chem., Int. Ed.,* 2003, **43**, 210.

[9] P. Chaudhuri, *Coord. Chem. Rev.,* 2003, **243**, 143.

[10] F. E. Mabbs and D. J. Machin, *Magnetism and Transition Metal Complexes*, Chapman and Hall (London), 1973.

[11] C. J. Milios, S. Piligkos and E. K. Brechin, *Dalton Trans*., 2008, 1809.

[12] (a) I.D. Brown and D. Altermatt, *Acta Crystallogr.,* 1985, *B* **41**, 244; (b) H.H. Thorp, *Inorg. Chem*., 1992, **31**,1585; (c) W. Liu and H. H Thorp, *Inorg. Chem*., 1993, **32**, 4102; (d) J. P. Naskar, S. Hati and D. Datta, Acta *Crystallogr.,* 1997, **B53**, 885.

[13] J. J. Borras-Alemnar, J. M. Clemente-Juan, E. Coronado and B. S. Tsukerblat, *J. Comp. Chem*., 2001, **22**, 985.

[14] (a) S. Carretta, T. Guidi, P. Santini, G. Amoretti, O. Pieper, B. Lake, J. Van Slageren, H. Mutka, M. Russina, C. J. Milios and E. K. Brechin. *Phys. Rev. Lett*., 2008, **100**, 157203; (b) S. Bahr, C. J. Milios, E. K. Brechin ,V.Mosser and W. Wernsdorfer, *Phys. Rev. B*, 2008, **78**, 132401.

[15] S. Piligkos, "MAGMOFIT", The University of Copenhagen.

[16] (a) S. Piligkos, J. Bendix, H. Weihe, C. J. Milios and E. K. Brechin., *Dalton Trans*., 2008, 2277; (b) A. Bencini and D. Gatteschi, *EPR of Exchange Coupled Systems*, Springer, Berlin, 1990.

[17] W. Wernsdorfer, *Adv. Chem. Phys.,* 2001, **118**, 99.

[18] M. Mola, S. Hill, P. Goy and M. Gross, *Rev. Sci. Instrum*., 2001, **71**. 186 .

[19] S. Takahashi and S. Hill, *Rev. Sci. Inst*., 2005, **76**, 023114.

[20] S. Takahashi, R. S. Edwards, J. M. North, S. Hill and N. S. Dalal, *Phys. Rev. B,* 2004, **70**, 094429.

[21] S. Datta, E. Bolin, C. J. Milios, E. K. Brechin and S. Hill, submitted to *Polyhedron*.

[22] S. Datta *et al.,* in preparation

[23] See for example: (a) D. Gatteschi, O. Kahn and R. D. Willett, Eds. *Magneto-Structural Correlations in Exchange Coupled Systems*; D. Reidel: Dordrecht, 1985; (b) W. H. Crawford, H. W. Richardson, J. R. Wasson, D. J. Hodgson and W. E. Hatfield, *Inorg. Chem.,* 1976, **15**, 2107; (c) W. E. Hatfield, *Comments Inorg. Chem.,* 1981, **1,** 105; (d) J. Glerup, D. J Hodgson and E. Petersen, *Acta Chem. Scand.* 1983, **A37**, 161; (e) M. F. Charlot, O. Kahn and M. Drillon, *Chem. Phys.,* 1982, **70**, 177; (f) W. E. Marsh, K. C. Patel, W. E. Hatfield and D. J. Hodgson, *Inorg. Chem.,* 1983, **22**, 511; (g) C. P. Landee and R. E.Greeney, *Inorg. Chem.,* 1986, **25**, 3371; (h) S. S.Tandon, L. K. Thompson, M. E. Manuel and J. N. Bridson, *Inorg. Chem.* 1994, **33**, 5555; (i) S. M. Gorun and S. J. Lippard, *Inorg. Chem.* 1991, **30,** 1625; (j) H. Weihe and H. U Güdel, *J. Am. Chem. Soc.* 1997, **119**, 6539.

[24] (a) T. Cauchy, E. Ruiz and S. Alvarez, *J. Am. Chem. Soc.,* 2006, **128**, 15722; (b) F. Neese, *J. Am. Chem. Soc.,* 2006, **128**, 10213; (c) M. R. Pederson and S. N. Khanna, *Phys. Rev. B*, 1999, **59**, 693 R; (d) A. V. Postnikov, J. Kortus and M. R. Pederson, *Physica Status Solidi*, 2006, **243**, 2533; (e) K. Isele, F. Gigon, A. F. Williams, G. Bernardinelli, P. Franz and S. Decurtins, *Dalton Trans.* 2007, 332; (f) M. A. Halcrow, J.-S. Sun, J. C. Huffman and G. Christou, *Inorg. Chem.,* 1995, **34**, 4167 ; (g) J. M. Clemente-Juan, B. Chansou, B. Donnadieu and J.-P.Tuchagues, *Inorg. Chem.,* 2000, **39**, 5515.

[25] (a) T. C. Stamatatos, D. Foguet-Albiol, S.-C. Lee, C. C. Stoumpos, C. P. Raptopoulou, A. Terzis, W. Wernsdorfer, S. Hill, S. P. Perlepes and G. Christou, *J. Am. Chem. Soc*. 2007, **129**, 9484. (b) C. Lampropoulos, K. A. Abboud, T. C. Stamatatos and G. Christou, *Inorg. Chem.*, 2009, **48**, 813.

[26] (a) J. B. Vincent, H. R. Chang, K. Folting, J. C. Huffman, G. Christou and D. N. Hendrickson, *J. Am. Chem. Soc*., 1987, **109**, 5703-5711; (b) R. D. Cannon and R. P. White, *Prog. Inorg. Chem.,* 1988, **36**, 195.

[27] L. F. Jones, R. Inglis, M. E. Cochrane, K. Mason, A. Collins, S. Parsons, S. P. Perlepes and E. K. Brechin, *Dalton Trans*., 2008, 6205.

[28] E. Ruiz, J. Cano, C. J. Milios and E. K. Brechin, unpublished results.

[29] (a) R. Inglis, L. F. Jones, K. Mason, A. Collins, S. A. Moggach, S. Parsons, S. P. Perlepes, W. Wernsdorfer and E. K. Brechin, *Chem. Eur. J*., 2008, **14**, 9117; (b) R. Inglis, L.F. Jones, G. Karotsis, A. Collins, S. Parsons, S. P. Perlepes, W. Wernsdorfer and E. K. Brechin, *Chem. Commun*., 2008, 5924.

[30] (a) C. J. Milios, A. Vinslava, A. G. Whittaker, S. Parsons, W. Wernsdorfer, G. Christou, S. P. Perlepes and E. K. Brechin, *Inorg. Chem.*, 2006, **45**, 5272; (b) C. J. Milios, R. Inglis, R. Bagai, W. Wernsdorfer, A.

Collins, S. Moggach, S. Parsons, S. P. Perlepes, G. Christou and E. K. Brechin, *Chem. Commun.*, 2007, 3476; (c) L. F. Jones, M. E. Cochrane, B. D. Koivisto, D. A. Leigh, S. P. Perlepes, W. Wernsdorfer and E. K. Brechin, *Inorg. Chim. Acta*, 2008, **361**, 3420.

[31] D. J. Watkin, C. K. Prout, J. R. Carruthers, P. W. Betteridge and R. I. Cooper, *CRYSTALS,* Issue 12, 2003, Chemical Crystallography Laboratory, University of Oxford: Oxford, UK.